

Highly Efficient Corrosion Inhibition of Carbon Steel in Aggressive Acidic Media with a Pyridazinium-based Ionic Liquid

Sami BEN AOUN*

Department of Chemistry, Faculty of Science, Taibah University, PO. Box 30002 Al-Madinah Al-Munawarah, KSA

*E-mail: sbenaoun@taibahu.edu.sa; Tel. +966-590-900-727 ; Fax. +966-4847-0235

Received: 29 May 2013 / Accepted: 12 June 2013 / Published: 1 August 2013

The inhibitive effect of 1-benzylpyridazin-1-ium bromide ionic liquid (MS20) on the corrosion of carbon steel in molar HCl has been investigated by means of weight loss measurements, kinetics and thermodynamics studies. A marked decrease of the corrosion rate (CR) was observed with increasing MS20 concentration. An effective inhibition with ca. 91.3% efficiency (IE%) was reached at 1 mM inhibitor concentration. The effect of temperature showed an increasing (IE%) with increasing temperature reaching a peak value of ca. 97.5% at 343 K. Results clearly revealed that MS20 inhibition activity proceeds via a chemisorption leading to the formation of a very strongly-adsorbed protective layer that blocks both the anodic and cathodic sites of carbon steel which synergistically hindered both the hydrogen evolution reaction and the carbon steel surface dissolution. The adsorption of MS20 onto the carbon steel surface followed a Langmuir isotherm.

Keywords: Corrosion inhibitors, Hydrochloric acid, Ionic liquids, Gravimetric analysis, Absorption.

1. INTRODUCTION

Protection against corrosion, the electrochemical destruction of metallic structures occurring through gradual anodic dissolution, represents a vital concern for many industries. This phenomena is typically favored on less noble metals (mainly iron, aluminum, copper, zinc, magnesium and their alloys) when exposed to corrosive environment such as acids. Hydrochloric acid is widely used in removing scale and salts from steel surfaces, cleaning tanks and pipelines and steel alloys [1].

Over the years, tremendous efforts have been deployed aiming at finding suitable organic and inorganic corrosion inhibitors in various corrosive media [2-8]. Most effective are organic compounds

containing functional groups that incorporate sulfur, oxygen, nitrogen, phosphorous, aromatic rings and π -electrons in their structures [9-12].

It has been proven that several factors contribute to the driving force of the inhibitory action of such compounds e.g. types of functional groups, number and type of adsorption sites, charge distribution, molecular structure, molecular size and molecular mass [13, 14].

Nitrogen-containing compounds constitute one of the most widely investigated type of corrosion inhibitors. This includes: azoles [15-22], substituted aniline-N-salicylidenes [23], amides [24], quaternary ammonium salts [25-32], polyamino-benzoquinone polymers [33], cationic surfactants [34, 35], and heterocyclic compounds [36, 37]. It was shown that nitrogen atom's strong adsorption onto the metal surface induces the formation of a protective layer resulting in increasing corrosion inhibition with increasing concentration which in some cases reaches 99% efficiency [27, 38, 39]. Accordingly, nitrogen-containing compounds, especially heterocyclic ones, are considered as effective corrosion inhibitors. Other authors worked on sulfur-containing inhibitors [26–31].

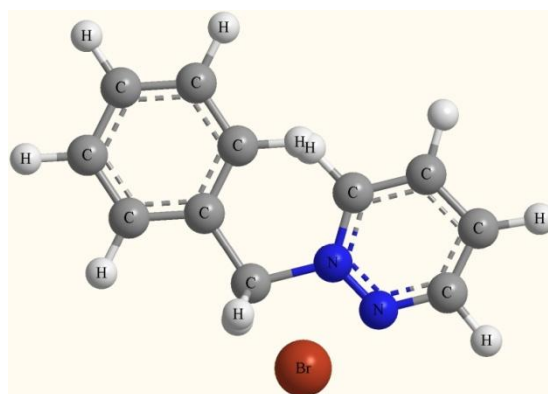
On the other hand, and despite the very interesting properties of ionic liquids (ILs) [40-51] and their wide range of applications [52-56], these eco-friendly compounds have received little interest as corrosion inhibitors. It has been reported that some ILs based on imidazolium, pyridinium and pyridazinium exhibited corrosion inhibition properties for the corrosion of various metals [57-67].

The present work aims at investigating the corrosion inhibition of carbon steel in 1 M HCl solution by means of a pyridazinium-based ionic liquid, namely the (1-benzylpyridazin-1-ium bromide). The effect of IL concentration on the corrosion inhibition efficiency (IE%) will be examined.

The effect of temperature on (IE%) will be investigated as well, leading to the understanding of the inhibition process kinetics and thermodynamics. Explanations concerning the mode of inhibition will be formulated accordingly.

2. EXPERIMENTAL

2.1. Chemicals, materials and equipments:



Scheme 1. Structure of 1-benzylpyridazin-1-ium bromide (MS20)

Microwave-assisted synthesis and characterization of various imidazolium-based, piridinium-based and pyridazinium-based ionic liquids (ILs) was reported in details by M. Messali et al. [64, 65, 68-70]. The structure of the investigated (IL) in the current work, namely the (1-benzylpyridazin-1-ium bromide) is shown in scheme 1. In the following text, this compound will be denoted as (MS20) for simplicity.

The aggressive corrosion media (i.e. molar HCl solution) was prepared by diluting the necessary volume of a stock concentrated hydrochloric acid solution (Fisher Scientific Ltd.). The necessary amount of the investigated MS20 was dissolved in the same media in order to prepare concentrations in the range 10^{-6} to 10^{-3} mol. L⁻¹. Ethanol (99.8%, Sigma-Aldrich) and Acetone (99.5%, Panreac) were used for the cleaning of carbon steel specimen. Carbon steel of 0.5 mm thickness (purchased from Sami Belal Est., Al-Madinah Al-Munawarah) was precisely cut into (2.5 cm × 3.0 cm) specimens.

The working temperature was controlled by means a water bath (GFL-1031, Gesellschaft Labortechnik, Germany). Precise weighing of studied specimens was made using a digital analytical semi-micro balance (GR-202, A&D Co. Ltd., Japan).

2.2. Weight loss measurements:

The carbon steel specimens were electrochemically cleaned, then degreased and polished to a mirror-like finish. The cut sheets of ca. 15 cm² surface area were thoroughly cleaned with distilled water, dried with ethanol and stored in desiccators till the experiments. The volume of the corrosion solution (with and without MS20) was kept constant at ca. 50 mL. The immersion time was chosen to be 5 hours and all experiments were carried out at room temperature (constantly maintained at ca. 296 K ± 1 K) unless otherwise specified. At the end of each experiment, the carbon steel specimen was washed with a copious amount of distilled water then with acetone to ensure the removal of all corrosion products and finally cleaned and dried with ethanol before weighing.

All experiments were duplicated to ensure reproducibility and the mean values are reported in the current work.

2.3. Kinetics and Thermodynamics:

For these studies, the effect of temperature on various corrosion parameters was studied in the range 296-343 K. Further details will be discussed in coming sections.

3. RESULTS AND DISCUSSION

3.1. Gravimetric study:

The gravimetric study allows the calculation of several corrosion parameters [67, 68, 71] by means of the mathematical relationships given below. The corrosion rate (CR) of carbon steel investigated in this study was calculated using the following equation:

$$CR = \frac{\Delta m}{At} \quad (1)$$

Δm is the weight loss ($m_i - m_f$) in mg with m_i and m_f being the initial and final masses of the carbon steel specimen, before and after corrosion tests, respectively. A (cm^2) is the exposed surface area of the specimen and t (h) is its immersion time in the investigated solution. The corrosion rate (CR) is therefore measured in ($\text{mg}\cdot\text{cm}^{-2}\cdot\text{h}^{-1}$)

The inhibition efficiency (IE%) can therefore be defined by the equation:

$$IE\% = \left[1 - \frac{CR^0 - CR^i}{CR^0} \right] \times 100 \quad (2)$$

CR^0 and CR^i are the corrosion rates in the absence and presence of inhibitor, respectively.

From the measurements of the inhibition efficiency, the fractional surface coverage (θ) can be determined as per the equation:

$$\theta = \frac{IE\%}{100} \quad (3)$$

The obtained data at room temperature (i.e. 296 K) is tabulated in table 1 for inhibitor concentrations ranging from “blank” to 10^{-3} M. A very clear concentration dependence of the corrosion rate (CR) (and therefore inhibition efficiency (IE%) and fractional surface coverage (θ)) is depicted.

Table 1. Gravimetric results for the corrosion parameters of carbon steel corrosion in 1 M HCl with various concentrations of MS20 obtained at 296 K.

[MS20] ($\text{mol}\cdot\text{L}^{-1}$)	CR ($\text{mg}\cdot\text{cm}^{-2}\cdot\text{h}^{-1}$)	IE%	θ
Blank	0.199	-----	-----
10^{-6}	0.170	14.7	0.417
10^{-5}	0.107	46.2	0.462
10^{-4}	0.038	80.9	0.809
10^{-3}	0.017	91.3	0.913

The inhibition efficiency reaches a maximum value of ca. 91.3 % in the presence of 10^{-3} M MS20 showing the effectiveness of the latter as a corrosion inhibitor for carbon steel in the present work conditions. This is better visualized in figure 1 that shows the significant decrease in the corrosion rate (CR) upon addition of MS20 to the aggressive corrosion solution to reach a minimum value when as less as 1 mM MS20 concentration is attained.

This tremendous change in the corrosion rate values had a very strong impact on the inhibition efficiency, which in its turn increases with increasing MS20 concentrations as depicted from table 1 and plotted in figure 2 reaching the highest value of ca. 91.3 % at an MS20 concentration of 10^{-3} M.

A plausible explanation of these results is that the increasing inhibitor's concentrations reduces the carbon steel exposed surface to the corrosion media through the increasing number of adsorbed molecules on its surface which hinders the direct acid attack on the metal surface [72]. Unveiling the nature of this adsorption phenomenon is necessary to understand the inhibition mechanism of the investigated MS20 compound.

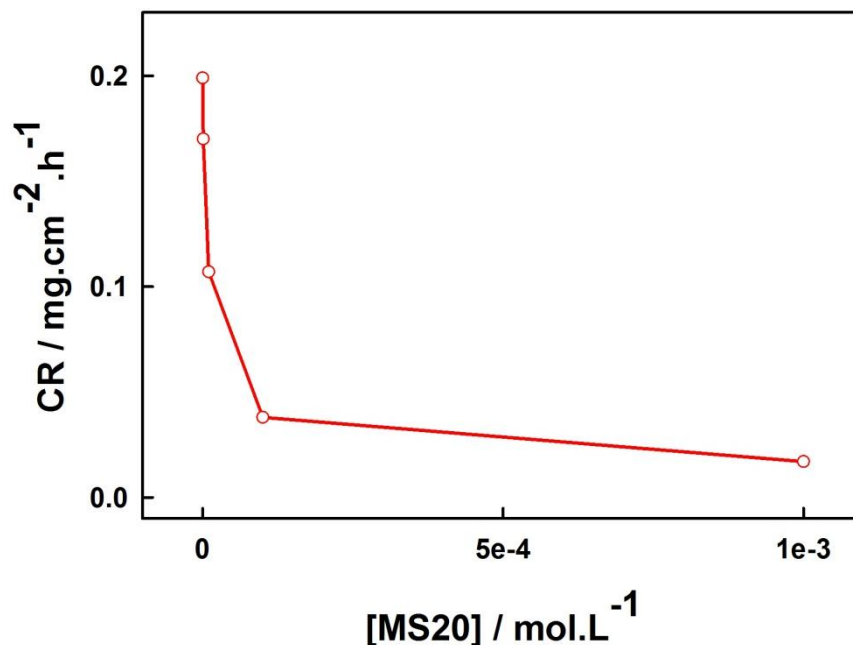


Figure 1. Variation of the corrosion rate (CR) of carbon steel with the concentration of MS20 in 1 M HCl at 296 K.

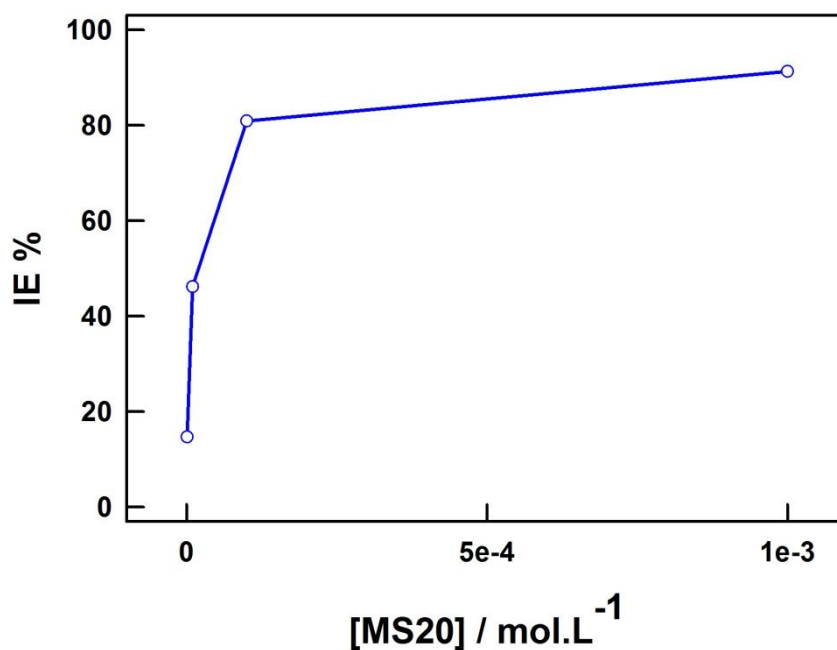


Figure 2. Variation of the inhibition efficiency (IE%) of carbon steel corrosion with the concentration of MS20 in 1 M HCl at 296 K.

3.2. Kinetics and thermodynamics:

The kinetics of the corrosion rate of carbon steel as a function of MS20 concentration might be assumed to obey the following equation [73]:

$$\log CR = \log k + B \log [MS20] \quad (4)$$

with k being the rate constant ($\text{mg. cm}^{-2} \cdot \text{h}^{-1}$) and B is the reaction constant which is a measure of the inhibitor efficiency in this case.

A plot of Log CR against log [MS20] based on the data given in table 2 is displayed in figure 3. The resulting graph has a good linearity ($R^2 = 0.981$) showing that the kinetic parameters can indeed be calculated using equation (2). The values of B (calculated from the slope of the graph) and k (derived from the y-intercept) are given in table 3 as well.

Table 2. Kinetic parameters of carbon steel corrosion in 1 M HCl with various concentrations of MS20 obtained at 296 K.

[MS20] (mol.L^{-1})	0	10^{-6}	10^{-5}	10^{-4}	10^{-3}
log [MS20]	-----	-6	-5	-4	-3
CR ($\text{mg.cm}^{-2} \cdot \text{h}^{-1}$)	0.199	0.170	0.107	0.038	0.017
Log CR	-0.701	-0.770	-0.971	-1.420	-1.770
B	-0.345				
k ($\text{mg.cm}^{-2} \cdot \text{h}^{-1}$)	1.64×10^{-3}				

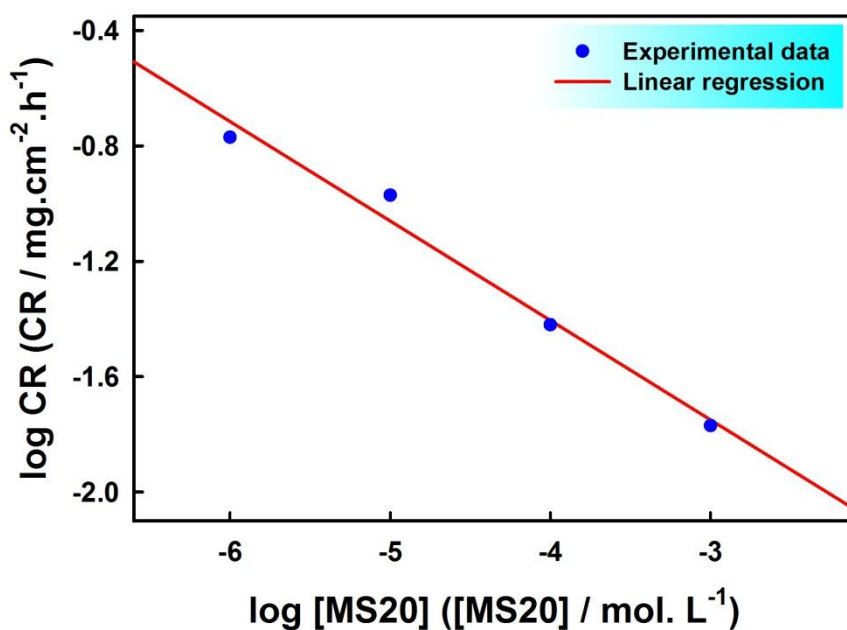


Figure 3. Variation of log CR with log [MS20] for carbon steel corrosion in 1 M HCl at 296 K.

It is noteworthy that the negative sign of the reaction constant reflect the inverse proportionality of the corrosion rate to the inhibitor concentration and its relatively high negative value reflects the good inhibitory properties of the investigated MS20 [73].

Temperature is a factor that plays an important role in the corrosion of a given material in a corrosive environment. The behavior of the former might be affected by temperature in addition to the possible modification in the metal-inhibitor interaction. It should be noted, however, that the temperature effect on the acid-metal inhibition reaction might be quite complex owing to the various changes occurring on the metal surfaces. For instance, rapid etching, inhibitor desorption and possible inhibitor decomposition [73, 74].

Carbon steel corrosion in acidic media is generally accompanied by the evolution of hydrogen gas, the amount of which is directly proportional to the temperature leading to higher corrosion rate at higher temperatures. Synergistically, the reactants energy to form the activated complex which in its turn dissociates to form the corrosion products increases with increasing temperature [75, 76].

In the present study, investigation of the influence of temperature on the corrosion rate in the absence and presence of 10^{-3} M MS20 as well as on the inhibition efficiency has been conducted in the temperature range (296 K–343 K) and results are reported in table 3.

Table 3. Gravimetric results for the corrosion parameters of carbon steel corrosion in 1 M HCl in the absence (CR^0) and presence (CR^i) of 10^{-3} M MS20 obtained at different working temperatures.

T (K)	CR^0 (mg.cm ⁻² .h ⁻¹)	CR^i (mg.cm ⁻² .h ⁻¹)	IE%	θ
296	0.199	0.017	91.3	0.913
313	0.835	0.047	94.3	0.943
323	2.221	0.080	96.4	0.964
333	4.946	0.132	97.3	0.973
343	10.875	0.277	97.5	0.975

Examination of the results shown in table 3 reveals that the corrosion rate in all cases increases with increasing temperature, as expected. From this table, the figure 4 was plotted.

An eye-catching feature in figure 4 is that the acceleration of the corrosion rate with increasing temperature is far low in the presence of 10^{-3} M MS20 compared with inhibitor-free solution. In fact, while the corrosion rate reaches an extreme value of ($CR^0 =$ ca. 10.875 mg.cm⁻².h⁻¹) at 343 K in the blank 1 M HCl compared with its initial value of ($CR^0 =$ ca. 0.199 mg.cm⁻².h⁻¹), this behavior is almost ten-fold lower in the presence of 10^{-3} M MS20 where the corrosion rate increased from ($CR^i =$ ca. 0.017 mg.cm⁻².h⁻¹) to ($CR^i =$ ca. 0.277 mg.cm⁻².h⁻¹) only.

A very interesting feature depicted in table 3 is the increase of the inhibition efficiency with increasing temperature which is of practical interest in processes requiring the protection of the material at high temperature[77]. A maximum value of ca. 97.5% was reached in the present study at 343 K as displayed in figure 5.

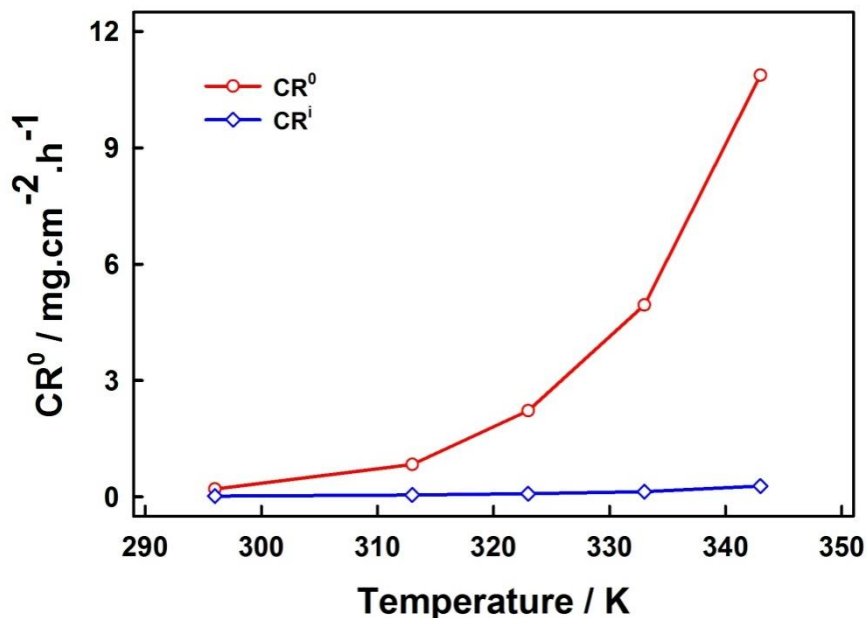


Figure 4. Effect of temperature on the corrosion rate of carbon steel in 1 M HCl in the absence (CR^0) and the presence (CR^i) of 10^{-3} M MS20.

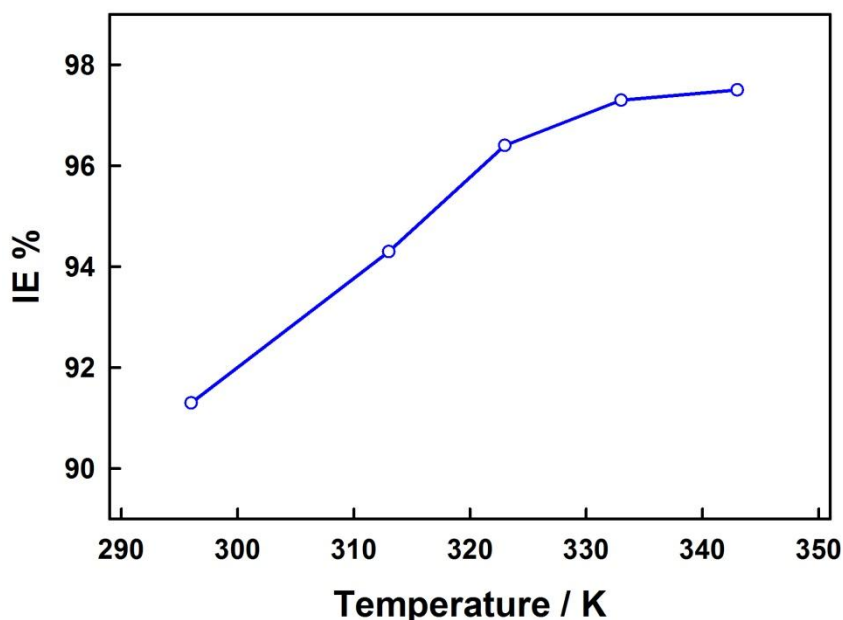


Figure 5. Effect of temperature (296 K–343 K) on the inhibition efficiency (IE%) of carbon steel corrosion in a (10^{-3} M MS20 + 1 M HCl) solution.

Similar increase in the inhibition efficiency has been observed in literature at several metals, like copper [78], aluminum [77] and steel [73, 79-81]. The most probable interpretation of this behavior is that the inhibition mechanism proceeds through a chemical adsorption (chemisorptions) of MS20 molecules onto the carbon steel surface and this indeed increases with rising temperature [73].

Further thermodynamic/kinetic investigations follow with the aim to evaluate the adsorption parameters and elucidate the corrosion/inhibition mechanisms.

The apparent activation thermodynamic parameters, namely the activation energy (E_a), the activation enthalpy (ΔH_a) and the activation entropy (ΔS_a) of the corrosion process under study can be calculated [67, 71, 82] using Arrhenius equation:

$$CR = A \exp \left[-\frac{E_a}{RT} \right] \quad (5)$$

And the alternative formulation of Arrhenius equation, the transition-state equation:

$$CR = \frac{RT}{Nh} \exp\left(\frac{\Delta S_a}{R}\right) \exp\left(-\frac{\Delta H_a}{RT}\right) \quad (6)$$

where A ($\text{mg}\cdot\text{cm}^{-2}\cdot\text{h}^{-1}$) is the Arrhenius pre-exponential factor, R is the universal gas constants ($8.3144621 \text{ J}\cdot\text{K}^{-1}\cdot\text{mol}^{-1}$), N is Avogadro’s number ($6.02252 \times 10^{23} \text{ mol}^{-1}$) and h is Plank’s constant ($6.626176 \times 10^{-34} \text{ J}\cdot\text{s}$).

A plot of $\ln(CR)$ against $(1/T)$ gives a straight line as displayed in figure 6.

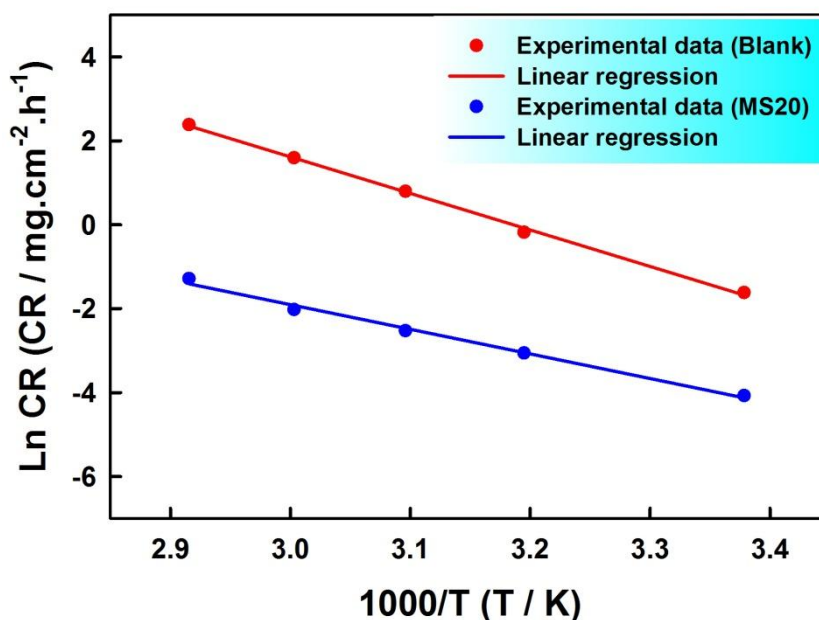


Figure 6. Arrhenius plots for carbon steel corrosion rates (CR) in 1 M HCl in the presence and absence of 10^{-3} M MS20.

The value of (A) was calculated from the y-intercept of respective lines. The slopes of these plots ($-E_a/RT$) yielded the values of the activation energy (E_a) both in the absence and presence of the inhibitor. All results are tabulated in table 4.

Table 4. Corrosion thermodynamic parameters for carbon steel in 1 M HCl with and without 10^{-3} M MS20

	Fig.6 slope	Fig.6 intercept	Fig.7 slope	Fig.7 intercept	A (mg.cm ⁻² .h ⁻¹)	E _a kJ.mol ⁻¹	ΔH _a kJ.mol ⁻¹	ΔS _a kJ.mol ⁻¹
Blank	-8.701	27.725	-8.384	20.962	1.099×10^{12}	72.340	69.705	-23.266
MS20	-5.866	15.695	-5.548	8.932	6.550×10^6	48.770	46.126	-123.279

And a plot of Ln(CR/T) against (1/T) is displayed in figure 7 for the corrosion of carbon steel in 1 M HCl in both the absence and presence of 10^{-3} M MS20. Each obtained straight line has a slope of $(-\Delta H_a/R)$ and an intercept of $(\text{Ln}[R/Nh] + \Delta S_a/R)$ from which the values of ΔH_a and ΔS_a were calculated, respectively. These results are tabulated in table 4, as well.

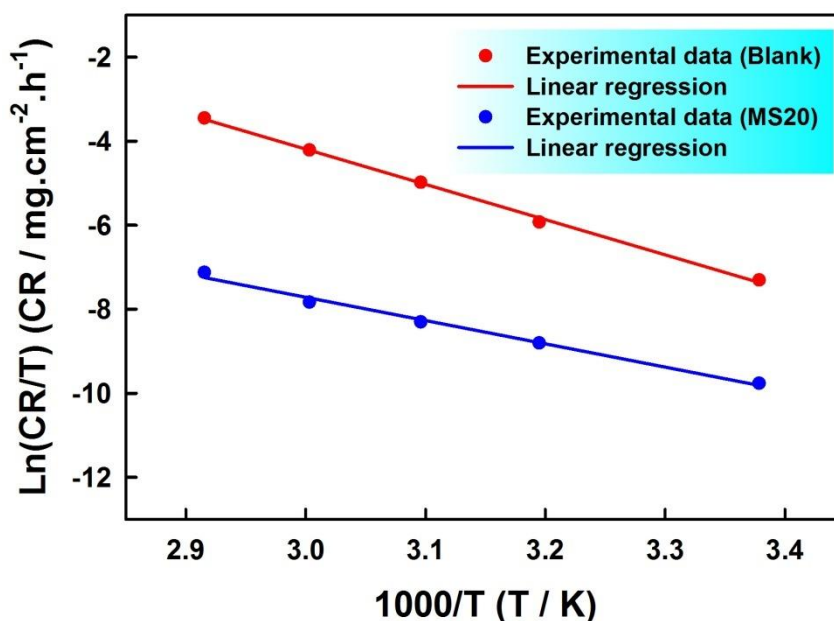


Figure 7. Transition-state plots for carbon steel corrosion rates (CR) in 1 M HCl in the presence and absence of 10^{-3} M MS20.

The significant decrease in the apparent activation energy in the presence of inhibitor is a prove that the inhibitory effect of the investigated MS20 for carbon steel corrosion in 1 M HCl proceeds indeed via a chemisorption [73, 80]. The same tendency applies to the Arrhenius pre-exponential factor as similarly observed in other studies [73, 79, 83, 84]. This increase in the value of the pre-exponential factor (A) induces the increase of the corrosion rate (CR) showing that the investigated (MS20) compound is a highly effective inhibitor since it shows high inhibition efficiency even at low activation energy.

Another observation is that, for both blank and MS20-containing solution, the values of ΔH_a are lower than the values of the respective activation energies which corresponds to a decrease in the total

reaction volume due to a gaseous process which is nothing but the hydrogen evolution reaction. Very interestingly the difference of the two values is almost constant with an average value of ca. 2.64 kJ.mol⁻¹ which is very close to the average value of the product (RT) in the investigated temperature range. Such behavior is characteristic of a unimolecular gas-phase reaction obeying the following equation [73, 80]:

$$E_a - \Delta H_a = RT \quad (7)$$

The last parameter given in table 4, the entropy of activation (ΔS_a), bears a negative sign for both blank and inhibitor-containing media. This is typical of an association-based formation of the activated complex in the rate determining step of the reaction mechanism. In other words, an increased ordering on forming the activated complex [85].

3.3. Adsorption isotherm:

The mechanism of inhibition of carbon steel corrosion by MS20 is tightly related to the adsorption of the inhibitor molecules onto the carbon steel surface [86-88] and this can be investigated using the adsorption isotherm. It is well documented that this phenomena is dependent, in one hand, on the nature and charge of the metal, and in the other hand, on the chemical structure and the distribution of charge in the inhibitor molecule, in addition to the type of electrolyte [89-94]. In this respect, two main categories are generally distinguished: chemical adsorption (chemisorption) and physical adsorption (physisorption) according to the thermodynamic parameters obtained from the adsorption isotherm.

A great variety of adsorption isotherms might be used to assess the behavior of corrosion inhibitors. The most frequently used are Langmuir, Temkin, Frumkin and Freundlich isotherms [73, 95] given by the following equations:

Temkin isotherm

$$\{\exp (f \cdot \theta)\} = K_{ads} \cdot C_{inh} \quad (8)$$

Langmuir isotherm

$$\left\{ \frac{\theta}{1-\theta} \right\} = K_{ads} \cdot C_{inh} \quad (9)$$

Frumkin isotherm

$$\left\{ \frac{\theta}{1-\theta} \right\} \{\exp (-2f \cdot \theta)\} = K_{ads} \cdot C_{inh} \quad (10)$$

Freundlich isotherm

$$\theta = K_{ads} \cdot C_{inh} \quad (11)$$

Where C_{inh} is the bulk concentration of the investigated inhibitor, K_{ads} is its adsorption equilibrium constant and f is the Temkin heterogeneity factor ($f = -2\alpha$), α being the Frumkin lateral interaction factor describing the molecular interactions in the adsorbed layer.

The experimental data is in excellent agreement with the Langmuir adsorption isotherm with a very good correlation coefficient ($R^2 = ca. 0.9999$) for the plot C_{inh}/θ against C_{inh} as shown in figure 8.

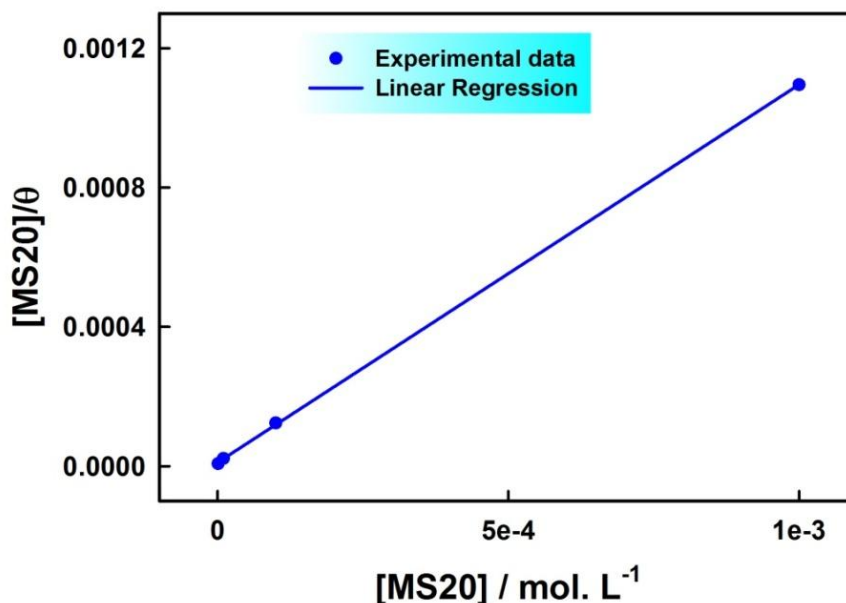


Figure 8. Langmuir adsorption isotherm of MS20 on carbon steel surface in 1 M HCl at 296 K.

The slope equals almost unity and the reciprocal of the intercept gives the value of the adsorption equilibrium constant (K_{ads}) which can be used to calculate the value of the Gibbs free energy of adsorption using the following equation [75]:

$$\Delta G_{ads} = -RT \ln(55.5 K_{ads}) \quad (12)$$

(55.5 is the value of the molar concentration of water in the solution [96]). Results are tabulated in table 5.

Table 5. Thermodynamic parameters for the adsorption of MS20 onto the carbon steel surface in 1 M HCl

Inhibitor	Slope	K_{ads} (mol ⁻¹ .L)	R^2	ΔG_{ads} (kJ.mol ⁻¹)
MS20	1.085	96.432×10^3	0.9999	-38.13

The negative value of the adsorption free energy as shown in table 5 gives a double indication: the first is the spontaneity of the adsorption process and the second is the strong adsorption of the MS20 inhibitor onto the carbon steel surface and therefore its high stability [75, 80, 97-99].

Moreover, there is a great deal of reports concerning the value of the adsorption free energy which in general falls into one of two ranges describing the general modes of adsorption, namely chemical adsorption (chemisorption) and physical adsorption (physisorption) [94, 100-109].

The former pertains to charge sharing or transfer from the organic species, in this case the corrosion inhibitor, to the corroding metal surface which results in the formation of a coordinate type bonding. And this is characterized by values of $|\Delta G_{\text{ads}}| \leq 20 \text{ kJ. mol}^{-1}$.

While, the latter describes a process that is due to an electrostatic interaction between the charged metal surface and the charged molecules. In that case the value of the adsorption free energy falls in the range $|\Delta G_{\text{ads}}| \geq 40 \text{ kJ. mol}^{-1}$.

In the current study, the obtained value is $\Delta G_{\text{ads}} = \text{ca. } -38.127 \text{ kJ.mol}^{-1}$ which is very close to -40 kJ.mol^{-1} , suggesting that the adsorption mode is predominantly a chemisorption. Similar descriptions were reported for N-naphtyl N'-phenylthiourea ($\Delta G_{\text{ads}} = \text{ca. } -38.78 \text{ kJ.mol}^{-1}$) [80], thiourea ($\Delta G_{\text{ads}} = \text{ca. } -39 \text{ kJ.mol}^{-1}$) [110] and mercapto-triazole ($\Delta G_{\text{ads}} = \text{ca. } -32 \text{ kJ.mol}^{-1}$) [111].

A plausible explanation of this chemisorption in terms of corrosion mechanism would be the adsorption of MS20 molecules onto both anodic and cathodic sites of the corroding carbon steel surface [80]. The adsorption on the cathodic site would result from the existence of the MS20 as cationic species which is in fact very obvious for the investigated ionic liquid (cf. the structure of MS20). This will hinder to some extent the hydrogen evolution reaction. This was in fact visualized during the carried experiments. While, the adsorption of this compound onto the anodic sites would be driven by the lone electron pairs of nitrogen and the π -electrons of C=N and C=C, which will diminish the dissolution of carbon steel.

4. CONCLUSION

In this study, we investigated the inhibitory effect of a pyridazinium-based ionic liquid (1-benzylpyridazin-1-ium bromide) abbreviated here as MS20. Very interestingly, an effective corrosion inhibition was obtained for carbon steel in 1 M HCl in the presence of MS20. The results of gravimetric, kinetics and thermodynamics investigations enabled the understanding of the inhibition process and the determination of various characteristic parameters. These results can be summarized as follows:

- MS20 showed a high inhibition efficiency (IE%) that increases with increasing inhibitor concentration.
- An MS20 concentration of as low as 10^{-3} M was enough to hinder the corrosion of carbon steel with an efficiency (IE% = ca. 91.3%).
- The kinetic study showed the good inhibitory properties of MS20 and enabled to calculate of the kinetic rate constant of the inhibition process ($k = \text{ca. } 0.451 \text{ mg.cm}^{-2}.\text{h}^{-1}$).

- From the study of the effect of temperature, it was found that (IE%), very interestingly, increased with increasing temperature reaching a peak at 343 K (IE% = ca. 97.5%) which is of a practical interest in several industrial processes.
- Thermodynamic investigations confirmed that MS20 inhibition process followed a Langmuir isotherm and that the MS20 action proceeds via a spontaneous chemisorption of the inhibitor onto the carbon steel surface resulting in the formation of quite a strong coordinate type bonds.
- MS20 is likely to adsorb on both anodic and cathodic sites of the corroding carbon steel surface reducing simultaneously the hydrogen evolution reaction (HRR) and the dissolution of the metal.

ACKNOWLEDGMENT

S. Ben Aoun thanks Prof. M. Messali for providing the MS20 compound for testing. The partial financial support to this work from the Deanship of Scientific Research, Taibah Univeristy (Project No. 658/432) is acknowledged.

References

1. I. Ahamad, R. Prasad, M.A. Quraishi, *Corros. Sci.*, 52 (2010) 3033-3041.
2. M. Bouklah, B. Hammouti, M. Benkaddour, T. Benhadda, *J. Appl. Electrochem.*, 35 (2005) 1095-1101.
3. A. Fiala, A. Chibani, A. Darchen, A. Boulkamh, K. Djebbar, *Appl. Surf. Sci.*, 253 (2007) 9347-9356.
4. A.S. Fouda, A.A. Al-Sarawy, E.E. El-Katori, *Desalination*, 201 (2006) 1-13.
5. I. Ahamad, R. Prasad, M.A. Quraishi, *Corros. Sci.*, 52 (2010) 1472-1481.
6. D.K. Yadav, B. Maiti, M.A. Quraishi, *Corros. Sci.*, 52 (2010) 3586-3598.
7. S. Edrah, S.K. Hasan, *J. Appl. Sci. Res.*, 6 (2010) 1045-1049.
8. Y.J. Tan, S. Bailey, B. Kinsella, *Corros. Sci.*, 38 (1996) 1681-1695.
9. M. Dahmani, A. Et-Touhami, S.S. Al-Deyab, B. Hammouti, A. Bouyanzer, *Intern. J. Electrochem. Sci.*, 5 (2010) 1060-1069.
10. A.Y. Musa, A.A.H. Kadhum, A.B. Mohamad, M.S. Takriff, A.R. Daud, S.K. Kamarudin, *Corros. Sci.*, 52 (2010) 526-533.
11. E.M. Sherif, S.M. Park, *J. Electrochem. Soc.*, 152 (2005) B428-B433.
12. E.M. Sherif, S.M. Park, *Electrochim. Acta*, 51 (2006) 1313-1321.
13. A. Radi, B. Hammouti, S. Radi, *J. Mater. Environ. Sci.*, 1 (2010) 96.
14. H.A. El-Dahan, T.Y. Soror, R.M. El-Sherif, *Mater. Chem. Phys.*, 89 (2005) 260-267.
15. O. Benali, L. Larabi, M. Traisnel, L. Gengembre, Y. Harek, *Appl. Surf. Sci.*, 253 (2007) 6130-6139.
16. E.S.H.E. Ashry, A.E. Nemr, S.A. Essawy, S. Ragab, *Progress in Organic Coatings*, 61 (2008) 11-20.
17. K.F. Khaled, *Electrochim. Acta*, 48 (2003) 2493-2503.
18. A. Popova, *Corros. Sci.*, 49 (2007) 2144-2158.
19. A. Popova, M. Christov, S. Raicheva, E. Sokolova, *Corros. Sci.*, 46 (2004) 1333-1350.
20. A. Popova, M. Christov, A. Zwetanova, *Corros. Sci.*, 49 (2007) 2131-2143.
21. V.S. Sastri, J.R. Perumareddi, M. Lashgari, M. Elboudjaini, *Corrosion*, 64 (2008) 283-288.

22. K. Tebbji, A. Aouniti, A. Attayibat, B. Hammouti, H. Oudda, M. Benkaddour, S. Radi, A. Nahle, *Indian J. Chem. Technol.*, 18 (2011) 244-253.
23. J.D. Talati, M.N. Desai, N.K. Shah, *Mater. Chem. Phys.*, 93 (2005) 54-64.
24. T. Tüken, B. Yazici, M. Erbil, *Turk. J. Chem.*, 26 (2002) 735-742.
25. S.M. Beloglazov, Z.I. Dzhafarov, V.N. Polyakov, N.N. Demushia, *Protection of Metals USSR*, 27 (1991) 810-813.
26. A.V. Fokin, M.V. Pospelov, A.N. Levichev, *Protection of Metals (English translation of Zashchita Metallov)*, 19 (1983) 242-244.
27. A.H. Nahlé, *Corrosion Prevention and Control*, 44 (1997) 99-105.
28. A.H. Nahlé, *Corrosion Prevention and Control*, 45 (1998) 124-130.
29. A. Nahle, *Bull. Electrochem.*, 18 (2002) 105-110.
30. A. Nahle, F.C. Walsh, *Corrosion Prevention and Control*, 42 (1995) 30-34.
31. B.V. Savithri, S.M. Mayanna, *Indian J. Chem. Technol.*, 3 (1996) 256-258.
32. T. Vasudevan, S. Muralidharan, S. Alwarappan, S.V.K. Iyer, *Corros. Sci.*, 37 (1995) 1235-1244.
33. S. Muralidharan, K.L.N. Phani, S. Pitchumani, S. Ravichandran, S.V.K. Iyer, *J. Electrochem. Soc.*, 142 (1995) 1478-1483.
34. H.A. Al-Lohedan, E. Khamis, Z.A. Issa, *Adsorpt. Sci. Technol.*, 13 (1996) 137-152.
35. L.G. Qiu, A.J. Xie, Y.H. Shen, *Mater. Chem. Phys.*, 91 (2005) 269-273.
36. A.A.A. Fattah, E.M. Mabrouk, R.M.A. Elgalil, M.M. Ghoneim, *Bull. Soc. Chim. Fr.*, 1 (1991) 48-53.
37. S.L. Granese, B.M. Rosales, C. Oviedo, J.O. Zerbino, *Corros. Sci.*, 33 (1992) 1439-1453.
38. A. Nahlé, I. Abu-Abdoun, I. Abdel-Rahman, *Anti-Corros. Meth. Mater.*, 54 (2007) 244-248.
39. A. Nahlé, I. Abu-Abdoun, I. Abdel-Rahman, *Anti-Corros. Meth. Mater.*, 55 (2008) 217-224.
40. R.D. Rogers, K.R. Seddon, *Science*, 302 (2003) 792-793.
41. N. Jain, A. Kumar, S. Chauhan, S.M.S. Chauhan, *Tetrahedron*, 61 (2005) 1015-1060.
42. J.S. Wilkes, *Green Chemistry*, 4 (2002) 73-80.
43. H.L. Ngo, K. LeCompte, L. Hargens, A.B. McEwen, *Thermochim. Acta*, 357-358 (2000) 97-102.
44. P. Bonhte, A.P. Dias, N. Papageorgiou, K. Kalyanasundaram, M. Grätzel, *Inorg. Chem.*, 35 (1996) 1168-1178.
45. K.M. Dieter, C.J. Dymek Jr, N.E. Heimer, J.W. Rovang, J.S. Wilkes, *J. Am. Chem. Soc.*, 110 (1988) 2722-2726.
46. F. Endres, S. Zein El Abedin, *Phys. Chem. Chem. Phys.*, 8 (2006) 2101-2116.
47. R. Hagiwara, Y. Ito, *J. Fluorine Chem.*, 105 (2000) 221-227.
48. S.A. Forsyth, J.M. Pringle, D.R. MacFarlane, *Australian Journal of Chemistry*, 57 (2004) 113-119.
49. S. Zhang, N. Sun, X. He, X. Lu, X. Zhang, *J. Phys. Chem. Ref. Data*, 35 (2006) 4.
50. H. Zhao, *Chem. Eng. Commun.*, 193 (2006) 1660-1677.
51. T. Tsuda, C.L. Hussey, *Electrochemical Society Interface*, 16 (2007) 42-49.
52. Z. Hua, S.Q. Xia, P.S. Ma, *Chem. Technol. Biotechnol.*, 80 (2005) 1089-1096.
53. M.A.M. Ibrahim, M. Messali, *Prod. Finish.*, 76 (2011) 14.
54. T. Sato, T. Maruo, S. Marukane, K. Takagi, *J. Power Sources*, 138 (2004) 253-261.
55. F. Endres, *ChemPhysChem*, 3 (2002) 144-154.
56. M. Ue, M. Takeda, A. Toriumi, A. Kominato, R. Hagiwara, Y. Ito, *J. Electrochem. Soc.*, 150 (2003) A499-A502.
57. R. Gašparac, C.R. Martin, E. Stupnišek-Lisac, *J. Electrochem. Soc.*, 147 (2000) 548-551.
58. D.Q. Zhang, L.X. Gao, G.D. Zhou, *Corros. Sci.*, 46 (2004) 3031-3040.
59. S. Muralidharan, S. Venkatakrishna Iyer, *Anti-Corros. Meth. Mater.*, 44 (1997) 100-106.
60. S. Shi, P. Yi, C. Cao, X. Wang, J. Su, J. Liu, *Huagong Xuebao/Journal of Chemical Industry and Engineering (China)*, 56 (2005) 1112-1119.
61. Q.B. Zhang, Y.X. Hua, *Electrochim. Acta*, 54 (2009) 1881-1887.

62. N.V. Likhanova, M.A. Domínguez-Aguilar, O. Olivares-Xometl, N. Nava-Entzana, E. Arce, H. Dorantes, *Corros. Sci.*, 52 (2010) 2088-2097.
63. M.A. Quraishi, M.Z.A. Rafiquee, S. Khan, N. Saxena, *J. Appl. Electrochem.*, 37 (2007) 1153-1162.
64. M.A.M. Ibrahim, M. Messali, Z. Moussa, A.Y. Alzahrani, S.N. Alamry, B. Hammouti, *Portug. Electrochim. Acta*, 29 (2011) 375-389.
65. M. Messali, *J. Mater. Environ. Sci.*, 2 (2011) 174-185.
66. M.E. Palomar, C.O. Olivares-Xometl, N.V. Likhanova, J.B. Pérez-Navarrete, *J. Surfac. Deterg.*, 14 (2011) 211-220.
67. S. Ben Aoun, *Der Pharma Chemica*, 5 (2013) 294-304.
68. A. Zarrouk, M. Messali, M.R. Aouad, M. Assouag, H. Zarrok, R. Salghi, B. Hammouti, A. Chetouani, *J. Chem. Pharm. Res.*, 4 (2012) 3427-3436.
69. M. Messali, *Arab. J. Chem.*
70. A.F. Al-Ghamdi, M. Messali, S.A. Ahmed, *J. Mater. Environ. Sci.*, 2 (2011) 215-224.
71. Bouklah, O. Krim, M. Messali, B. Hammouti, A. Elidrissi, I. Warad, *Der Pharma Chemica*, 3 (2011) 283-293.
72. L. Afia, N. Rezki, M.R. Aouad, A. Zarrouk, H. Zarrok, R. Salghi, B. Hammouti, M. Messali, S.S. Al-Deyab, *Intern. J. Electrochem. Sci.*, 8 (2013) 4346-4360.
73. E.A. Noor, *Intern. J. Electrochem. Sci.*, 2 (2007) 996-1017.
74. F.Z. Bouanis, F. Bentiss, M. Traisnel, C. Jama, *Electrochim. Acta*, 54 (2009) 2371-2378.
75. M.R. Laamari, J. Benzakour, F. Berrekhis, A. Derja, D. Villemin, *Arab. J. Chem.*
76. N.A. Negm, A.M.A. Sabagh, M.A. Migahed, H.M.A. Bary, H.M.E. Din, *Corros. Sci.*, 52 (2010) 2122-2132.
77. G.K. Gomma, M.H. Wahdan, *Mater. Chem. Phys.*, 39 (1995) 209-213.
78. M.M. Antonijevic, M.B. Petrovic, *Intern. J. Electrochem. Sci.*, 3 (2008) 1-28.
79. X. Li, G. Mu, *Appl. Surf. Sci.*, 252 (2005) 1254-1265.
80. L. Larabi, O. Benali, Y. Harek, *Mater. Lett.*, 61 (2007) 3287-3291.
81. D. Ben Hmamou, M.R. Aouad, R. Salghi, A. Zarrouk, M. Assouag, O. Benali, M. Messali, H. Zarrok, B. Hammouti, *J. Chem. Pharm. Res.*, 4 (2012) 3489-3497.
82. O.L. Riggs, R.M. Hurd, *Corrosion*, 23 (1967) 252-260.
83. L. Tang, G. Mu, G. Liu, *Corros. Sci.*, 45 (2003) 2251-2262.
84. X. Li, L. Tang, *Mater. Chem. Phys.*, 90 (2005) 286-297.
85. S.S. Abd El Rehim, H.H. Hassan, M.A. Amin, *Mater. Chem. Phys.*, 70 (2001) 64-72.
86. S. Cheng, S. Chen, T. Liu, X. Chang, Y. Yin, *Mater. Lett.*, 61 (2007) 3276-3280.
87. N. Hackerman, *Corrosion*, 18 (1962) 332t-337t.
88. N. Hackerman, J.D. Sudbury, *J. Electrochem. Soc.*, 97 (1950) 109-116.
89. A. Popova, E. Sokolova, S. Raicheva, M. Christov, *Corros. Sci.*, 45 (2003) 33-58.
90. D.Q. Zhang, L.X. Gao, G.D. Zhou, K.Y. Lee, *J. Appl. Electrochem.*, 38 (2008) 71-76.
91. J. Uehara, K. Aramaki, *J. Electrochem. Soc.*, 138 (1991) 3245-3251.
92. S.L. Granese, *Corrosion*, 44 (1988) 322-327.
93. A. Akiyama, K. Nobe, *J. Electrochem. Soc.*, 117 (1970) 999-1003.
94. B.G. Ateya, B.E. El-Anadouli, F.M. El-Nizamy, *Corros. Sci.*, 24 (1984) 509-515.
95. D. Do, Adsorption Analysis: Equilibria and Kinetics, Imperial College Press, 1980.
96. J. Flis, T. Zakroczymski, *J. Electrochem. Soc.*, 143 (1996) 2458-2464.
97. S.A. Ali, A.M. El-Shareef, R.F. Al-Ghamdi, M.T. Saeed, *Corros. Sci.*, 47 (2005) 2659-2678.
98. I. El Ouali, B. Hammouti, A. Aouniti, Y. Ramli, M. Azougagh, E.M. Essassi, M. Bouachrine, *J. Mater. Environ. Sci.*, 1 (2010) 1-8.
99. G. Avci, *Mater. Chem. Phys.*, 112 (2008) 234-238.
100. E. Khamis, F. Bellucci, R.M. Latanision, E.S.H. El-Ashry, *Corrosion*, 47 (1991) 677-686.

101. I.B. Obot, N.O. Obi-Egbedi, *Colloids and Surfaces A: Physicochemical and Engineering Aspects*, 330 (2008) 207-212.
102. M. Bouklah, B. Hammouti, M. Lagrenée, F. Bentiss, *Corros. Sci.*, 48 (2006) 2831-2842.
103. M. Bouklah, N. Benchat, B. Hammouti, A. Aouniti, S. Kertit, *Mater. Lett.*, 60 (2006) 1901-1905.
104. O.K. Abiola, N.C. Oforika, *Mater. Chem. Phys.*, 83 (2004) 315-322.
105. M. Özcan, R. Solmaz, G. Kardaş, İ. Dehri, *Colloids and Surfaces A: Physicochemical and Engineering Aspects*, 325 (2008) 57-63.
106. S. Hari Kumar, S. Karthikeyan, *J. Mater. Environ. Sci.*, 3 (2012) 925-934.
107. A. Zarrouk, H. Zarrok, R. Salghi, B. Hammouti, F. Bentiss, R. Tourir, M. Bouachrine, *J. Mater. Environ. Sci.*, 4 (2013) 177-192.
108. F.M. Donahue, K. Nobe, *J. Electrochem. Soc.*, 112 (1965) 886-891.
109. E. Bayol, A.A. Gürten, M. Dursun, K. Kayakirilmaz, *Acta Phys. Chim. Sin.*, 24 (2008) 2236-2243.
110. M. Metikoš-Huković, R. Basić, Z. Grubač, S. Brinić, *J. Appl. Electrochem.*, 26 (1996) 443-449.
111. H.-L. Wang, H.-B. Fan, J.-S. Zheng, *Mater. Chem. Phys.*, 77 (2003) 655-661.